

1 **Interaction between East Asian summer monsoon and ~~west~~**
2 **~~winds~~westlies as shown by tree-ring records**

3

4 ~~Shengchun Xiao^{1*}, Xiaomei Peng¹, Quanyan Tian¹, Aijun Ding², Jiali Xie¹, Jingrong~~
5 ~~Su^{1,3}~~

6 Xiao Shengchun^{1*}, Peng Xiaomei¹, Tian Quanyan¹, Ding Aijun², Xie Jiali¹, Su
7 Jingrong^{1,3}

8

9 ¹ Key Laboratory of Ecological Safety and Sustainable Development in Arid Lands,
10 Northwest Institute of Eco-Environment and Resources, Chinese Academy of
11 Sciences, Lanzhou, Gansu, China 730000.

12 ² College of Resources and Environment, Gansu Agricultural University, Lanzhou,
13 Gansu, China 730070.

14 ³ University of Chinese Academy of Sciences, Beijing, China 100049.

15 * Corresponding author (xiaosc@lzb.ac.cn).

16 Address: 320 West Donggang Road, Lanzhou City, Gansu Province, China.

17 Zip Code: 730000.

18

19 **Abstract:**

20
21 ~~Against the background of~~Atmospheric circulation changes, their driving mechanisms
22 and interactions are important topics in global ~~atmospheric circulation, local~~change
23 research. Local changes in the East Asian summer monsoon (EASM) and the mid-
24 latitude ~~westerly winds~~westerlies will inevitably affect the climate and ecology of the arid
25 zone of Northwest China. Hence, it is important to study these ~~changes~~regional
26 changes. While previous studies in this area are all single-point climate reconstruction
27 studies, there is a lack of research on the interaction areas and driving mechanisms of
28 the two major circulations. Dendroclimatology can provide high-resolution, long-term,
29 and reliable multi-point proxies for the study of inter-annual and inter-decadal climate
30 change. We chose to observe these changes in the Alxa Plateau using
31 dendrochronological methods. We assembled ring-width records ~~from~~of Qinghai
32 spruce ~~trees growing~~(*Picea crassifolia*) in the mountain regions surrounding the Alxa
33 Plateau: the Helan Mountains, Changling Mountain, and Dongdashan Mountain. ~~We~~
34 ~~analyzed these records for changes on interannual and interdecadal scales. Our~~The
35 results show that radial growth was indeed affected by changes in the
36 ~~monsoons~~monsoon and westerlies. The heterogeneity of precipitation and climatic wet-
37 dry changes in different regions is primarily influenced by the interactions between
38 atmospheric circulation systems, each with its own dominant controlling factors. In the
39 case of the Helan Mountains, both of these major atmospheric circulation systems play
40 a significant role in shaping climate changes. Changling Mountain in the southern part
41 of the Alxa Plateau ~~are~~is mainly influenced by the EASM. Dongdashan Mountain is
42 mainly influenced by the westerlies. Understanding these local conditions will help us
43 predict climate changes in Northwest China.

44
45 **Key words:** Alxa Plateau, dendroclimatology, ~~westerly winds~~westerlies, EASM,
46 interaction between winds and monsoon.

49 **1. Introduction**

50 **~~1.1 Importance of climate studies in northwestern China~~**

51 The alpine zone of Qinghai-Tibet, the arid zone of the northwestern interior, and
52 the humid zone of the east constitute the three main areas of China's natural
53 geomorphology (Chen et al., ~~2019b~~2019a). The Northwest China inland dry zone is
54 located in the hinterland of the Eurasian continent and is among the driest regions in
55 the world. It ~~exhibits~~displays typical ~~continental~~climatic characteristics: of a
56 continental climate. This region is mainly influenced by ~~westerly winds~~westerlies and the
57 EASM: (the East Asian summer monsoon). The interaction of these two factors results
58 in high precipitation variability and hence frequent droughts. This ~~would be the case~~was
59 true even before the onset of global climate change ~~began affecting in~~ the area; and it
60 is even more ~~the case~~pronounced in ~~current~~recent years. This inland ~~dry~~arid zone is
61 ~~very much an~~ecologically fragile ~~area~~ (Chen et al., 2019a; Chen et al., 2019b; Zhang
62 et al., 2023).

63 The semi-arid and arid regions of northern China are characterized by large areas
64 of sand and desert. They are the second largest source of dust in the world after the
65 Sahara. Their contribution to global climate change is large. So far inland, the influence
66 of the EASM is often weak (Zhang et al., 2021; Liu et al., 2022). It is opposed by the
67 ~~westerly winds~~westerlies that flow from the North Atlantic climate zone toward the
68 East Asian monsoon climate zone (Qu et al., 2004). The interaction between the
69 ~~westerly winds~~westerlies and the EASM governs precipitation, water vapor transport,
70 and thus the climate of northwestern China (Feng et al., 2004; Wang et al., 2005; Li et
71 al., 2008; Ma et al., 2011).

72 ~~It is important to understand the history of this interaction if we are to~~To estimate
73 ~~how the impact of~~ global climate change ~~will affect on~~ this interaction, it is crucial to
74 comprehend its historical context. Global atmospheric circulation is likely to change,
75 as is the EASM. Climate change will not only affect the regional climate and regional
76 water resources (Ding et al., 2023); it will affect East Asia (dust storms) and even the
77 rest of the globe. Hence, the study of climate in this region is of great practical and
78 theoretical significance (Chen et al., 2019a; Chen et al., 2019b).

79 The ~~westerly winds~~westerlies and the EASM meet at the northern boundary of the
80 Asian summer monsoon (Huang et al., 2023). In northern China, this boundary runs
81 from west to east, along the eastern section of the Qilian Mountains, the southern
82 foothills of the Helan Mountains, the Daqing Mountains, and the western section of the
83 Daxinganling Mountains. This is not a static boundary. It– fluctuates within a range of
84 200–700 km (Chen et al., 2018). It is important to understand the history of these
85 fluctuations (Huang et al., 2023).

86 This can be done using climate records such as lacustrine, eolian, and
87 dendrochronological (Sun et al., 2003; Liu et al., 2005; Li, 2009; Chen et al., 2010; Li
88 et al., 2016; Chen et al., 2019b; Qin et al., 2023). ~~Our research team specializes in~~
89 ~~dendrochronology, which~~Dendrochronology is one of the best tools for studying
90 paleoclimatic changes, due to its precise dating, high resolution, good continuity and
91 high replication (Zhang et al., 2003; Shao et al., 2010; Yang et al., 2014; Liu et al.,
92 2016).

93 94 **1.2 Previous work**

95 The climate history of the Baotou area, at the northern edge of the EASM, has been
96 studied at interannual and interdecadal scales for the past 260 years, based on June–
97 August precipitation reconstruction from tree-ring samples from the western Yinshan
98 Mountains (Liu et al., 2001; Liu et al., 2003). Using tree-rings and historical records,
99 Kang and Yang (2015) reconstructed the annual precipitation history of the East Asian
100 monsoon northern fringe zone for the last 530 years. They analyzed spatial variability
101 and possible driving mechanisms using the 400-mm isohyet.

102 Several May–July precipitation sequences have been reconstructed using ring-
103 width and latewood-width data from Chinese pine (*Pinus tabulaeformis*) growing in
104 the Helan Mountains (Ma et al., 2003; Liu et al., 2004; Chen et al., 2016). Studies of
105 tree-ring carbon and oxygen isotopes from Chinese pine samples have shown that $\delta^{18}\text{O}$
106 values increase with summer precipitation, while $\delta^{13}\text{C}$ values decrease (Zhang et al.,
107 2005a; Liu et al., 2008). ~~Westerly winds~~westerlies have also been shown to affect
108 precipitation in the Helan Mountains (Chen et al., 2010).

109 Principal component analysis of tree-ring chronologies constructed from data
110 collected at several sites in Gansu suggests that trees at these sites were more influenced
111 by EASM than by ~~west winds~~westerlies (Chen et al., 2013). These researchers also
112 found that the EASM weakened in 1970s, but recovered in the early 1990s. Tree-ring
113 data allowed the reconstruction of 330 years of PDSI (Palmer Drought Severity Index)
114 values for the Mount Hasi region (at the northern boundary of the summer monsoon
115 zone) (Kang et al., 2012). This study confirmed that radial growth of Chinese pine has
116 declined over the past three decades, due to the weakening of the EASM.
117 Dendrochronological reconstruction of precipitation in the Mount Changling region
118 (again using Chinese pine) suggested that precipitation in that region mainly depends
119 on the EASM (Chen et al. 2012). Other researchers have assembled tree-ring
120 chronologies from pines growing in the Mount Qilian region and the northern
121 mountains of the Hexi Corridor. Here again precipitation is associated with the EASM.
122 These chronologies have allowed scholars to compile precipitation, temperature, and
123 drought records for the last thousand years (Gou et al., 2015a; Gou et al., 2015b; Zhang
124 et al., 2017).

125 Most modern researchers studying climate change in the region are mostly carried
126 out on single sample sites (Wang et al., 2004; Liu et al., 2005; Chen et al., 2010; Chen
127 et al., 2016; Li et al., 2016; Liu et al., 2016; Chen et al., 2018). ~~There~~While, there is a
128 dearth of multi-site, regional, ~~large- and long time~~ scale studies on the interaction of the
129 westerlies and the EASM. ~~Our group compiled~~The research focuses on the interplay
130 area, and investigates the spatiotemporal heterogeneity in climate change and its
131 dominant driving factors, specifically related to the westerlies and East Asia monsoon
132 circulation in Alxa Plateau.

133 Compiled and analyzed tree-ring chronologies from Qinghai spruce (*Picea*
134 *crassifolia*) growing in the Helan, Changling, and Dongdashan mountain regions that
135 surround the Alxa Plateau, the climate response characteristics of spruce radial growth
136 in three regions was then analyzed. Combining the relevant Westerly and East Asia
137 monsoon circulation indices, the driving mechanism of the regional climate change by
138 with the interaction and synergistic roles of two atmospheric circulation systems in the

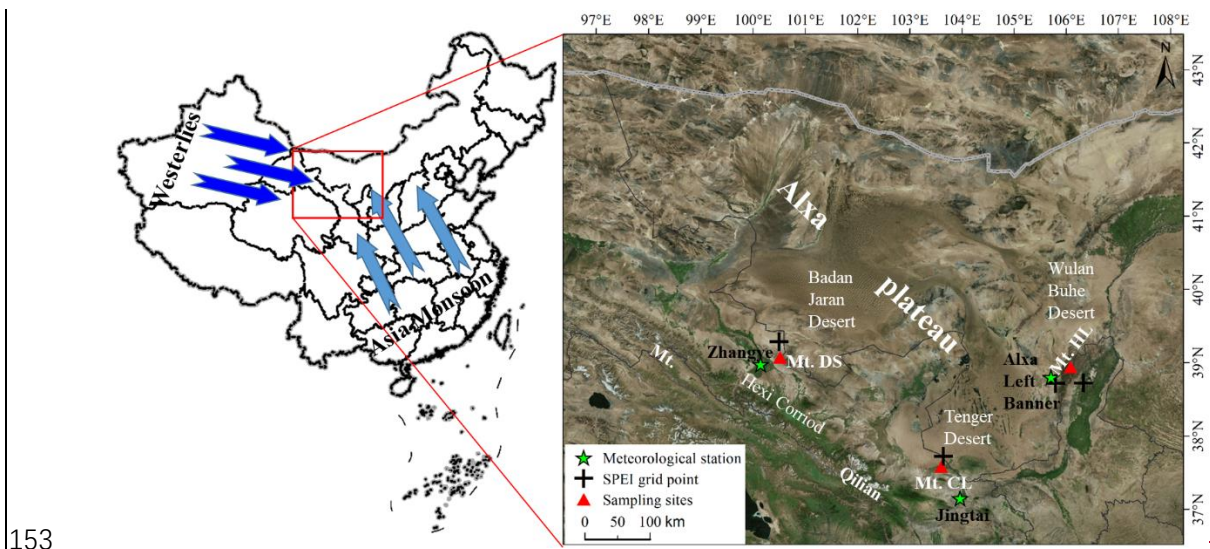
139 Alxa Plateau was explored. The results will lay a theoretical foundation for the climatic
140 evolution of the region and the desertification control.

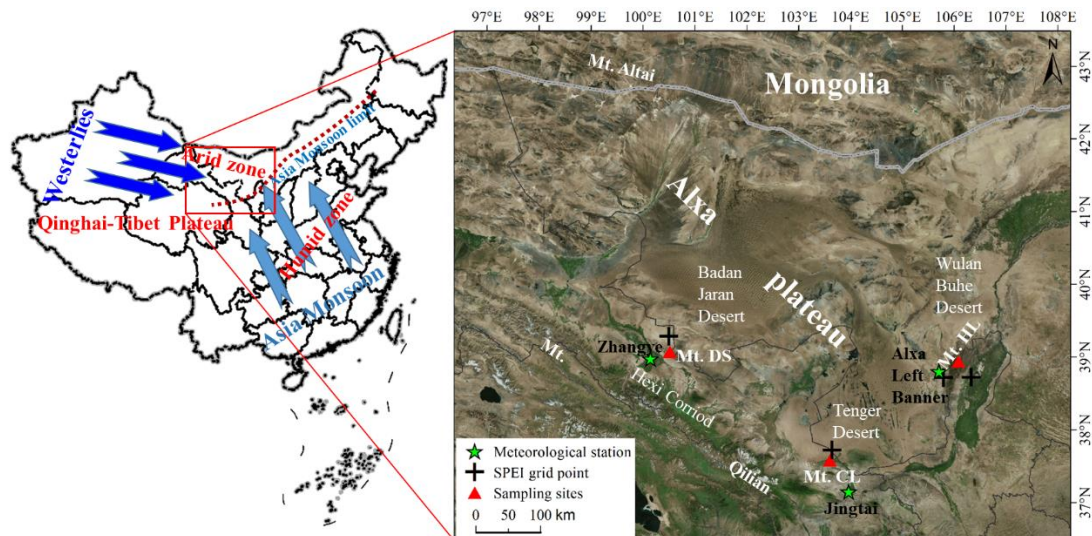
141

142 2. Material and methods

143 2.1 Study area

144 The Alxa Plateau is located in the western part of the Inner Mongolia Autonomous
145 Region and is surrounded by mountains (Fig.1). It consists primarily of three deserts:
146 Tengger, Ulan Buh, and Badan Jaran. It lies south of the Gobi desert. It is the main
147 source of the fierce sandstorms and dust storms that blow toward eastern China and the
148 Pacific. It has been much affected by climate change; sand- and dust storms have
149 increased, much to the detriment of lands to the east. The Chinese government is doing
150 what it can to establish an environmental defense line there. It is currently the Northern
151 Sand Prevention Belt of the National Two Ecological Barrier and Three Belts
152 Ecological Security Strategy Pattern (Xiao et al., 2017; Xiao et al., 2019).





154
 155 Figure 1. Location of tree-ring sampling sites and meteorological stations ~~(the right~~
 156 ~~panel is from Mapworld)~~

157
 158 There are several mountain ranges surrounding the Alxa Desert, such as the Helan
 159 Mountains in the east, the northern mountains of the Hexi Corridor, and the outliers of
 160 the Altai Mountains in the north. These mountains not only block the eastward and
 161 southward expansion of the desert (driven by high pressure regions from Mongolia);
 162 they are also the source of mountain rivers and streams that water the oases on the
 163 plateau.

164 The Alxa Plateau is located in the eastern margin of the inland arid region of Central
 165 Asia. It is affected not only by the mid-latitude westerly circulation, but also by the
 166 Asian monsoon and the plateau monsoon. It is in the zone where the mid-latitude
 167 westerly circulation and the Asian monsoon interact (Xiao et al., 2017; Chen et al.,
 168 2019b). As a result, there is large interannual variability of vegetation cover in the
 169 region (Ou and Qian, 2006; Tang et al., 2006; Li et al., 2013).

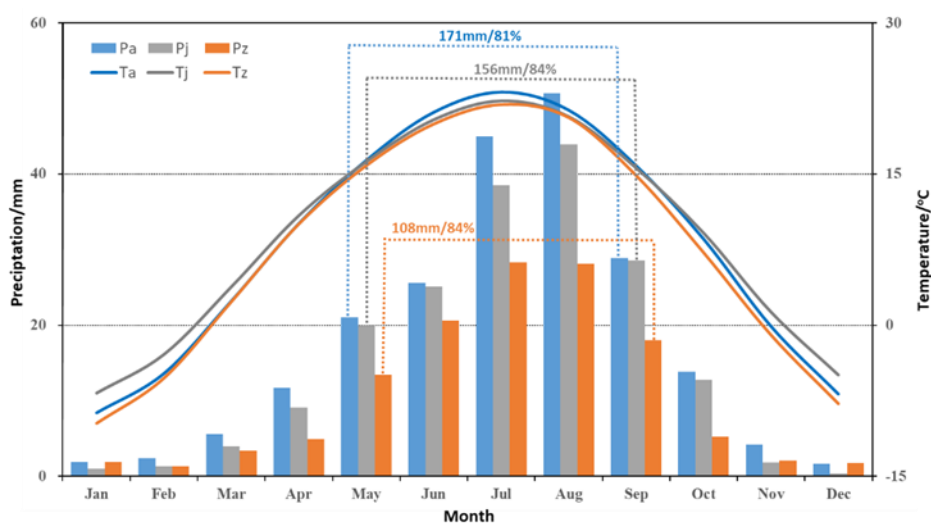
170 The Helan Mountains ($38^{\circ}27' \sim 39^{\circ}30'N$, $105^{\circ}20' \sim 106^{\circ}41'E$) (sampling site
 171 henceforth abbreviated as HL), are located at the eastern edge of the Tengger Desert.
 172 They stretch more than 200 kilometers from north to south; the main peak is $\sim 3,556$ m.
 173 The mountain forests are dominated by Qinghai spruce and Chinese pine, juniper,
 174 mountain aspen, and elm.

175 Mount Changling (37°12'~37°17', 102°45'~103°48'E) (sampling site henceforth
 176 abbreviated as CL) is an independent mountain protruding northward from the
 177 remnants of the eastern Qilian Mountains, ~~It~~ is located at the southern edge of the
 178 Tengger Desert; its elevations range from 2100 to 2900 m. The dominant tree species
 179 are Qinghai spruce and Chinese pine.

180 Mount Dongdashan (39°00'~39°04'N, 100°45'~100°51'E) (sampling site
 181 henceforth abbreviated as DS) is located at the southwestern edge of the Badan Jaran
 182 Desert and the middle part of Mount Qilian. It is one of the northern mountains along
 183 the Hexi Corridor; that range consists of mountains that vary from 2200 to 2637 m in
 184 elevation. Forests are dominated by Qinghai spruce and Qilian juniper.

185 The temperatures of the coldest months recorded at meteorological stations in the
 186 Alxa Left Banner (a division of the Alxa League region), Jingtai (a county in Gansu),
 187 and Zhangye (a city in Gansu) all occurred in January, ranging from -9.8°C to -6.8°C.
 188 The hottest months at those stations were in July (21.9 °C to 23.1 °C). These
 189 meteorological stations are the closest stations to our three sampling sites.

190 ~~Precipitation measured at those stations varied widely. The multi-year average of~~
 191 ~~total precipitation from May to September was 171 mm at Alxa Left Banner station,~~
 192 ~~156 mm at Jingtai station, and 108 mm at Zhangye station. This accounted for more~~
 193 ~~than 80% of the annual precipitation (Fig. 2).~~



194
 195 Figure 2. Climatic diagram of study area. Pa/Ta are the monthly total precipitation and
 196 monthly mean temperature at the Alxa Left Banner meteorological station (1953–2016);

197 Pj/Tj are the precipitation and temperature figures for the Jingtai meteorological station
198 (1957–2017); Pz/Tz are the precipitation and temperature figures for the Zhangye
199 meteorological station (1957–2017). The dashed box and appended data indicate the
200 total growing season precipitation in the study area and the proportion of total annual
201 precipitation.

202 Precipitation measured at those stations varied widely. The multi-year average of
203 total precipitation from May to September was 171 mm at Alxa Left Banner station,
204 156 mm at Jingtai station, and 108 mm at Zhangye station. This accounted for more
205 than 80% of the annual precipitation (Fig.2).

206

207 **2.2 Sample collection, processing and data analysis method**

208 **2.2.1 Sample collection, processing and dendrochronology construction**

209 Researchers used standard methods of tree-ring sample collection. One core was drilled
210 from each tree in the sample site. We collected 209 cores in total, from five sampling
211 sites at HL, 48 cores from one sampling site at CL, and 81 cores from two sampling
212 sites at DS. Relevant information ~~re~~of the sampling sites is summarized in Table 1.

213 Chronologies were constructed using standard dendrochronological methods-
214 (Cook, 1985). In order to highlight the high frequency signal, the RES chronology is
215 selected for later climate analysis. We calculated the highly significant correlations ($P <$
216 ≤ 0.001) between the chronologies of different points at the HL and DS mountains; a
217 weighting method was used to finally synthesize a chronology for each mountain.
218 Generally, the sub-sample signal strength (SSS) index and the mean series
219 intercorrelation (R_{bar}) are used to evaluate the credibility and quality of the chronologies.
220 The length of the reliable chronology is indicated by the parts of the series with a
221 subsample signal strength (SSS) index > 0.85 (Wigley et al., 1984). Another important
222 statistic is the mean series intercorrelation (R_{bar}), which is the mean correlation
223 coefficient among the ring series and is therefore an indication of the common variance.

224

225 **2.2.2 Climate data, atmospheric circulation indices and the related Analyzing** 226 **methods for chronological correlation**

227 Climate data for the study areas HL, CL, and DS were collected from the nearest
228 meteorological stations in Alxa Left Banner, Jingtai and Zhangye, respectively
229 (<http://data.cma.cn>).

230 We used SPEI ([Standardized Precipitation Evapotranspiration Index](#)) to represent
231 the local drought and wetness conditions, [which is widely used in the](#)
232 [dendrochronology studies and considering the effects of potential evapotranspiration,](#)
233 [precipitation and time scales \(Vicente-Serrano et al., 2010\)](#). SPEI data (grid-point
234 resolution 0.5°*0.5 °) was obtained from the grid-point datasets of the National Center
235 for Environmental Predictions-National Center for Atmospheric Research (NCEP-
236 NCAR). Time scales ranged from 1 month to 15 months. The mean values of data from
237 two grid-points closest to the HL sampling site (38.75°N, 105.75°E and 38.75°N,
238 106.25°E; period 1953–2015) were chosen for subsequent analysis. Grid-point data
239 from one site closest to our CL sampling site (37.75N, 103.75E; period 1951–2015)
240 was used for later analysis. Grid-point data from one site closest to our DS sampling
241 site (39.25°N, 100.75°E; period 1951–2015) was also used. As SPEI datasets are multi-
242 scale, we preprocessed the data to identify and select 11-month scaled SPEI datasets
243 for subsequent analysis.

244 We took into account the so-called lagging effect (the influence of fall and winter
245 climate factors on the radial growth of trees shows up later in the year) and chose to use
246 temperature, precipitation, and SPEI data from September of the previous year to
247 September of the current year (abbreviated as P9–P12 and C1–C9), as collected at each
248 meteorological station, for our climate response analysis.

249 The East Asian Summer Monsoon Index (EASMI) ([Li and Zeng 2005](#)) represents
250 the activity strength of the EASM. Larger EASMI values indicate a stronger summer
251 monsoon, smaller ones a weaker monsoon. In this study, the EASMI (mean values for
252 June–August in the period 1950–2017) defined by Li and Zeng (2005) was used to
253 study the impact of the EASM on climate change in the study area.

254 [The East Asian Summer Monsoon Index \(EASMI\) represents the activity strength](#)
255 [of the EASM. The East Asian summer monsoon \(EASM\) index is defined as an area-](#)
256 [averaged seasonally \(JJA\) dynamical normalized seasonality \(DNS\) at 850 hPa within](#)

257 the East Asian monsoon domain (10°-40°N, 110°-140°E) (Li and Zeng 2005). Larger
258 EASMI values indicate a stronger summer monsoon, smaller ones a weaker monsoon.
259 In this study, the EASMI (mean values for June–August in the period 1950–2017)
260 defined by Li and Zeng (2005) was used to study the impact of the EASM on climate
261 change in the study area.

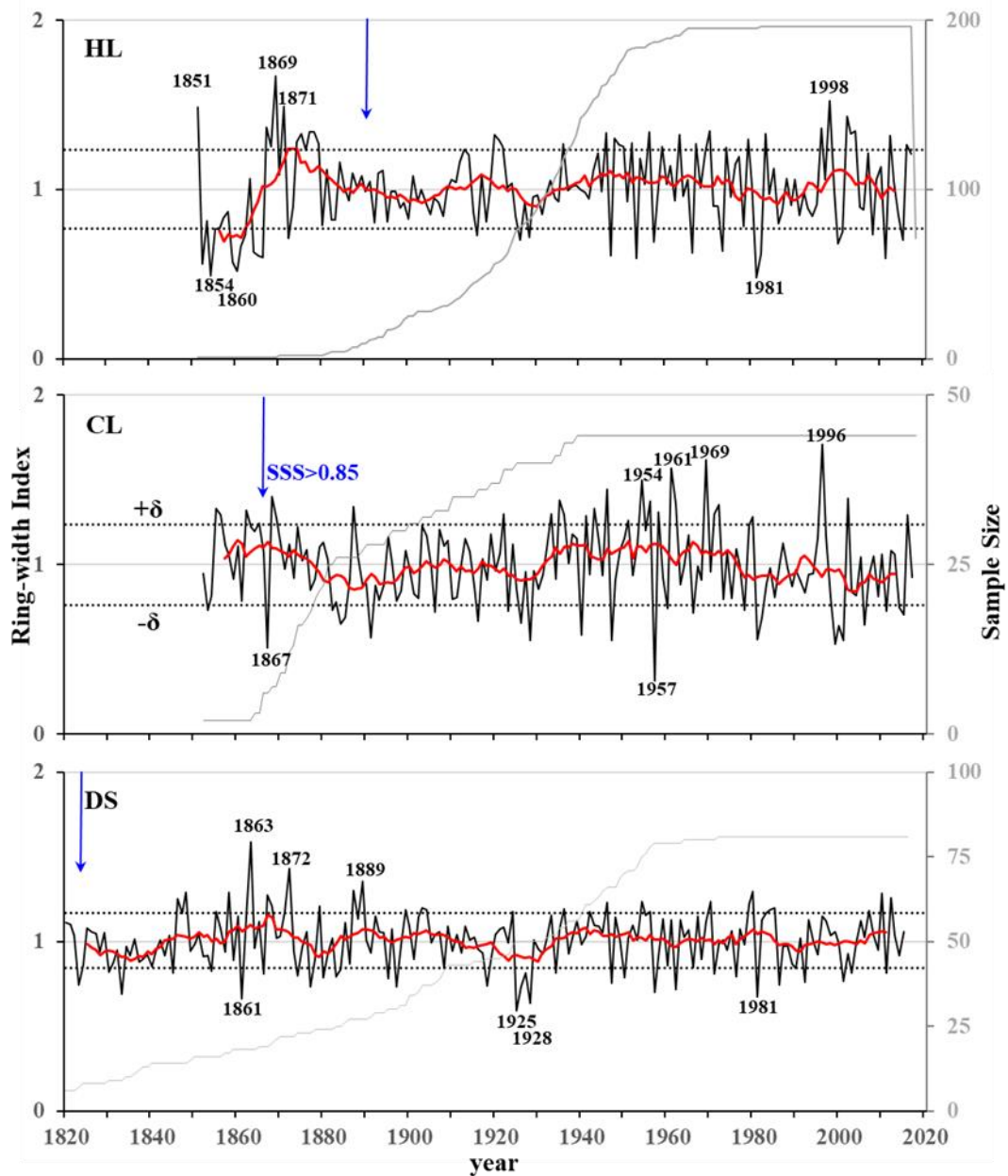
262 We used the Westerly Circulation Index (WCI annual mean; [https://cmdp.ncc-](https://cmdp.ncc-cma.net/cn/index.htm)
263 [cma.net/cn/index.htm](https://cmdp.ncc-cma.net/cn/index.htm)) to represent the strength of the mid-latitude westerlies. The
264 larger the WCI value, the stronger the Eurasian latitudinal circulation; the smaller the
265 value, the weaker the Eurasian latitudinal circulation. WCI data (period 1951–2015)
266 were derived from the Eurasian Latitudinal Circulation Index published by the National
267 Climate Center of the China Meteorological Administration ([https://cmdp.ncc-](https://cmdp.ncc-cma.net/cn/index.htm)
268 [cma.net/cn/index.htm](https://cmdp.ncc-cma.net/cn/index.htm)).

269 Interannual and interdecadal (sliding moving average of 11a) chrono-climatic/
270 cyclonic index correlation and partial correlation analyses were performed using SPSS
271 19.0. Based on the characteristics of tree-ring series, the sequences were classified into
272 three groups of low, average and high ring widths using $\text{mean} \pm 1\delta$ (SD δ : standard
273 deviation) as the classification criterion (with $\text{mean} \pm 2\delta$ as the extreme year).
274 Correlation statistical tests were performed with the corresponding annual circulation
275 indices; similar treatments and analyses were performed for the two major circulation
276 indices.

279 **3. Results and analysis**

280 **3.1 Ring-width chronologies and their characteristics**

281 Based on the sampling cores from five sample sites at HL, two sample sites at DS, and
282 one sample site at CL, ring-width residual chronologies were derived for each of the
283 three study areas (Fig. 3). Statistical parameters showed that the three chronologies
284 meet the usual requirements for correctly done dendrochronological studies: (Table 1).



285

286 Figure 3. Residual ring-width chronologies for the three study areas. The dark lines
 287 indicate the chronology; grey lines indicate the sample depth; red lines indicate the 11-
 288 year running mean chronology; dotted horizontal lines indicate the mean value $\pm 1\delta$,
 289 years with data identified as $>/< \text{mean} \pm 2\delta$ (δ : standard deviation); the blue arrows
 290 indicate the start of the reliable residual chronology ($\text{SSS} > 0.85$).

291

292 Table 1. Statistical characteristics of the sampling sites and the tree-ring chronologies.

293

294

Sampling sites	HL(5)	CL(1)	DS(2)
Latitude (°N)	38.52–38.97	37.61	39.04
Longitude (°E)	105.83–106.02	103.71	100.78
Elevation (m)	2200–2750	2490	2650–2700
Cores	209	48	81
Reliable period	1891–2018	1866–2017	1823–2015
MS	0.18–0.37	0.28	0.15–0.33
R_{bar}	0.45–0.61	0.56	0.40–0.60
SNR	22.5–56.1	38.9	25.7–42.5
EPS	0.96–0.98	0.98	0.96–0.98
PC1(%)	17.3–63.0	57.9	43.0–62.5

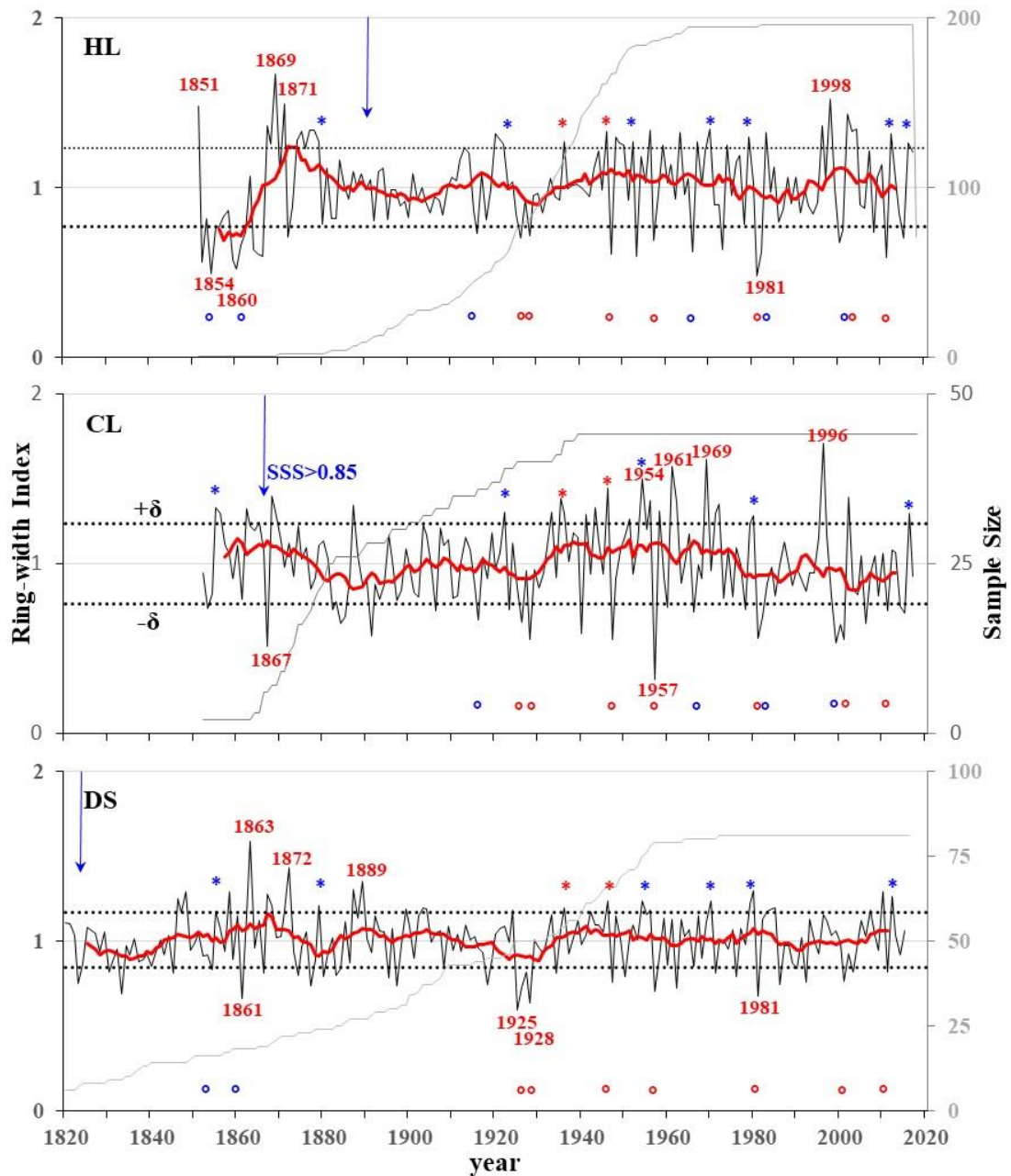
295 Reliable period; ($SSS > 0.85$), MS (mean sensitivity), R_{bar} (mean series intercorrelation), SNR (signal to
296 noise ratio), EPS (expressed population signal), and PC1 (variance explained by the first principal
297 component) refer to residual chronologies;).

298

299 3.2 Climate response characteristics

300 Correlation analysis comparing a) monthly mean temperature and precipitation at
301 neighboring meteorological stations and b) SPEI at the nearest grid-point showed that,
302 overall, the three residual chronologies were correlated negatively with monthly mean
303 air temperature, positively correlated with monthly precipitation, and positively
304 correlated with SPEI during the growing season (Fig. 4).–

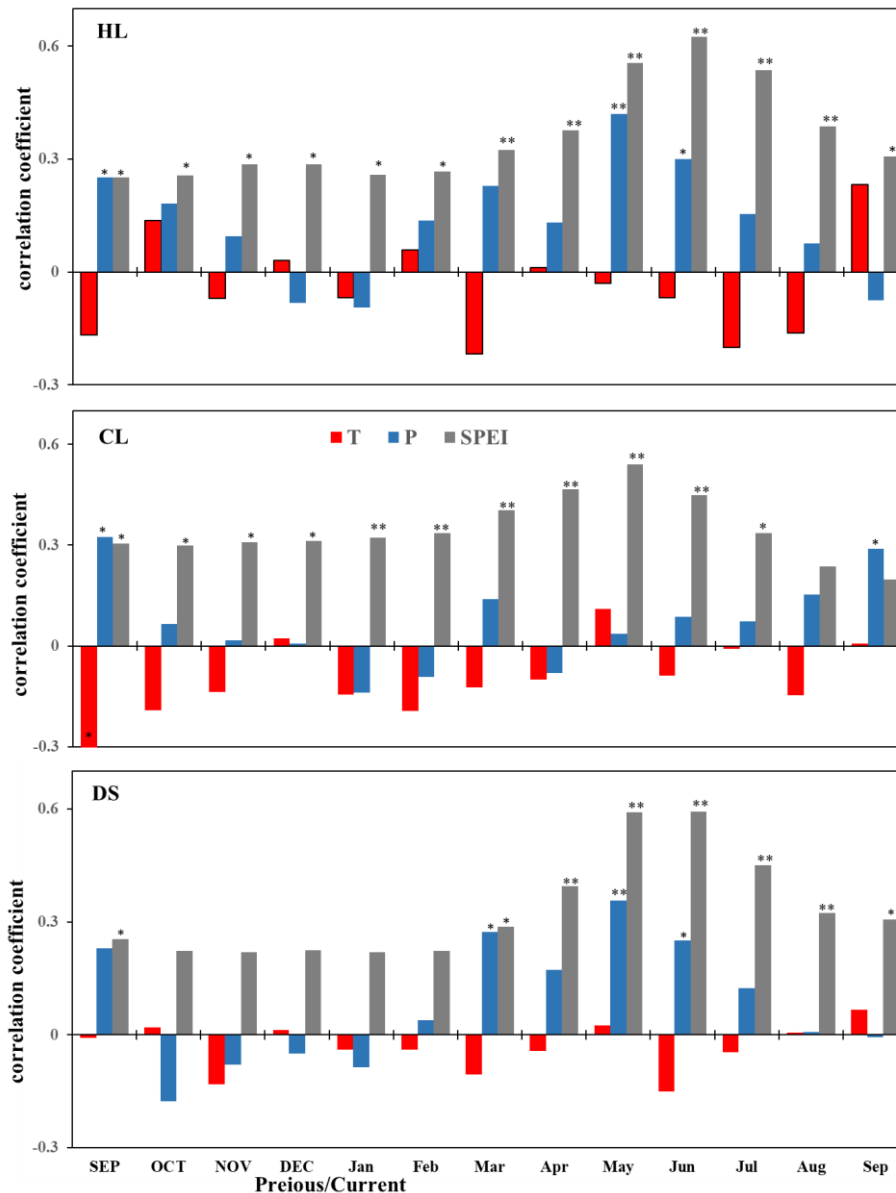
305 HL chronology was correlated negatively with mean temperature mainly in C5–C8
306 in the growing season, but not to the significant level. It was also positively correlated
307 with precipitation in all months except P12, C1, and C9, reaching significant levels ($P <$
308 ≤ 0.05) in P9, C5, and C6. All months were positively correlated with SPEI and reached
309 statistical significance ($P < \leq 0.05$), with C3–C8 showing highly significant correlation
310 levels ($P < \leq 0.01$).



311

312 Figure 3. Residual ring-width chronologies for the three study areas. The dark lines
 313 indicate the chronology; grey lines indicate the sample depth; red lines indicate the 11-
 314 year running mean chronology; dotted horizontal lines indicate the mean value $\pm 1\delta$;
 315 years with data identified as $>/< \text{mean} \pm 2\delta$ (δ : standard deviation); blue * and o indicate
 316 the years shared between two of the three sample sites, red * and o shows years shared
 317 between three sample sites; blue arrows indicate the start of the reliable residual
 318 chronology (SSS > 0.85).

319



320

321 Figure 4. Correlation coefficients (Pearson's r values) between the residual ring-width
 322 chronologies of Qinghai spruce at the three study areas (HL, CL and DS) and the observed monthly
 323 temperature (T), total monthly precipitation (P), and SPEI. * Pearson's r correlation, significant at
 324 P < 0.05. ** Pearson's r correlation, significant at P < 0.01. Month names of previous year are
 325 capitalized.

326 * Pearson's r correlation, significant at P < 0.05.

327 ** Pearson's r correlation, significant at P < 0.01.

328 Month names of previous year are capitalized.

329 CL chronology was negatively correlated with the mean temperature in almost
 330 months-except for P12, C5 and C9. Only P9, but only reached statistical significance

331 ~~($P < 0.05$)~~-a significant negative correlation ($P < 0.05$) with P9. CL chronology was
332 positively correlated with monthly precipitation, save for C1, C2, and C4. Only P9 and
333 C9 reached statistical significance ($P < 0.05$). All months were positively correlated
334 with SPEI, with P9–C7 reaching significant correlation levels ($P < 0.05$) and C1–C7
335 reaching highly significant correlation levels ($P < 0.01$).

336 DS chronology showed weak correlations between DS chronology and monthly
337 mean temperatures. None of the correlations reached levels of significance. DS
338 chronology was positively correlated with P9 and C2–C8 precipitation and reached
339 significant correlation levels for C3, C5, and C6 ($P < 0.05$). All months were positively
340 correlated with SPEI, with P9 and C3–C9 reaching significant correlation levels ($P < 0.05$)
341 and C4–C8 reaching highly significant correlation levels ($P < 0.01$).

342 Overall, the radial growth of Qinghai spruce at the three study areas seems to have
343 been limited, for the most part, by low precipitation during the growing season (April–
344 July). The three chronologies reflect regional wet and dry variations.

346 3.3 Regional climate changes as recorded by tree-ring widths

347 3.3.1 Regional climate change viewed at interannual scales

348 On interannual scales, the three residual chronologies, when compare, showed highly
349 significant correlations—(HL–CL: $n = 166$, $r = 0.04$, $P < 0.001$; HL–DS:
350 $n = 165$, $r = 0.331$, $P < 0.01$; 001; CL–DS: $n = 164$, $r = 0.374$, $P < 0.01$ 001). This
351 indicates that there was a high degree of consistency in the radial growth of Qinghai
352 spruce in the three regions.

353 According to the results of the chronology-climate response analysis in the
354 previous section, the high and low ring-width indices (mean $\pm 1\sim 2\delta$) of the chronology
355 at the three sample sites indicate wetter or drier, and extreme wet or dry years,
356 respectively (Table 2 Fig. 3).

357 Overall, the three ring-width residual chronologies (HL, CL, DS) had a total of two
358 shared wetter years and seven shared drier years. The HL and CL chronologies shared

359 four wet years and eleven dry years; the HL and DS chronologies shared five wet years
 360 and nine dry years; and the CL and DS chronologies shared five wet years and seven
 361 dry years (Table 2 Fig. 3).

362 **Table 2. Years of high or low growth, wet or dry climate in the three chronologies**

chronology	Higher index/wetness years ($\geq \text{mean} + 1\delta$)	Lower index/drought years ($\leq \text{mean} - 1\delta$)
HL	1851 , 1867, 1869 , 1871 , 1874, 1875, 1877, 1878, <u>1879</u> , 1920, 1921, <u>1922</u> , <u>1936</u> , <u>1946</u> , 1952, <u>1959</u> , 1963, 1967, <u>1970</u> , 1974, <u>1979</u> , 1983, 1996, 1998 , 2002, 2003, 2004, <u>2012</u> , <u>2016</u>	1852, 1854 , 1855, 1859, 1860 , <u>1861</u> , 1864, 1865, 1866, 1872, <u>1916</u> , <u>1926</u> , <u>1928</u> , <u>1947</u> , 1953, <u>1957</u> , <u>1966</u> , 1973, 1981 , <u>1982</u> , <u>2000</u> , <u>2001</u> , <u>2011</u>
CL	<u>1855</u> , 1862, <u>1922</u> , 1933, 1935, <u>1936</u> , 1941, <u>1946</u> , 1951, 1954 , 1958, 1961 , 1969 , 1972, <u>1980</u> , 1996 , <u>2016</u>	1867 , 1884, 1885, 1891, <u>1916</u> , 1923, <u>1926</u> , <u>1928</u> , <u>1947</u> , 1957 , 1960, <u>1966</u> , 1978, <u>1981</u> , <u>1982</u> , 1999, <u>2000</u> , <u>2001</u> , 2006, <u>2011</u> , 2014, 2015
DS	1846, 1848, <u>1855</u> , 1858, 1863 , 1867, 1868, 1872 , <u>1879</u> , 1887, 1889 , 1899, 1903, 1904, 1924, <u>1936</u> , 1942, <u>1946</u> , <u>1954</u> , 1956, <u>1959</u> , <u>1970</u> , <u>1979</u> , <u>1980</u> , 2007, 2010, <u>2012</u>	1823, 1830, 1833, <u>1854</u> , 1861 , 1874, 1877, 1880, 1883, 1884, 1895, 1897, 1908, 1925 , <u>1926</u> , 1927, 1928 , 1934, <u>1947</u> , 1950, <u>1957</u> , 1962, 1971, 1976, 1981 , 1985, 1990, 1992, <u>2001</u> , 2003, <u>2011</u>

363
 364 **Note: Bold is used to indicate extreme years ($> / < \text{mean} \pm 2\delta$; δ : standard deviation); double**
 365 **underlining indicates years shared between two of the three sample sites; bold underlining**
 366 **shows years shared between three sample sites.**

367 There were no extremely wet years shared by the three sample sites. However, there
 368 were two shared wetter years in 1936 and 1946 and several shared wetter years in later
 369 years among the three sample sites. For example, note the wetter years in 1922 and
 370 2016 for HL and DS chronologies; 1959, 1979, and 2012 for HL and DS chronologies;
 371 1855, 1954, and 1980 for CL and DS chronologies (Table 2 Fig. 3).

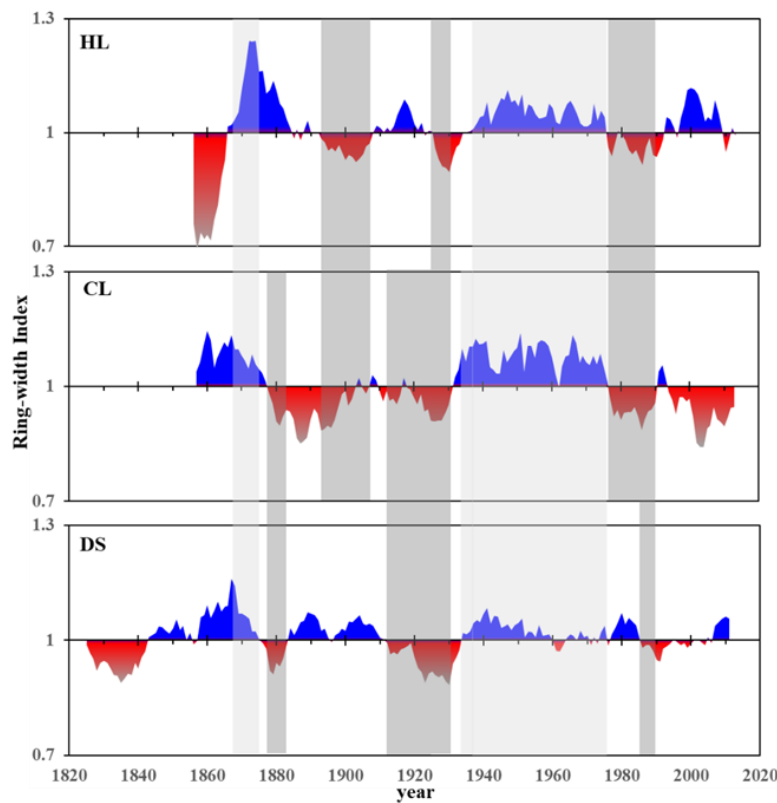
372 The extreme drought years are consistent among the three sample sites. For
 373 instance, there was an extreme drought year in 1981 at HL and DS sample sites; it was
 374 also a drought year at CL. An extreme drought year at CL in 1957 was also a drought
 375 year for the other two chronologies. Moreover, the extreme drought year of 1928 at DS

376 was a drought year at the other two sites. Drought years in 1926, 1947, 2001, and 2011
377 were seen in all three sites and in two of the three sample sites (1916, 1966, 1982, and
378 2000 at HL and CL; 1854 and 1861 at HL and DS) (Table 2 Fig. 3).

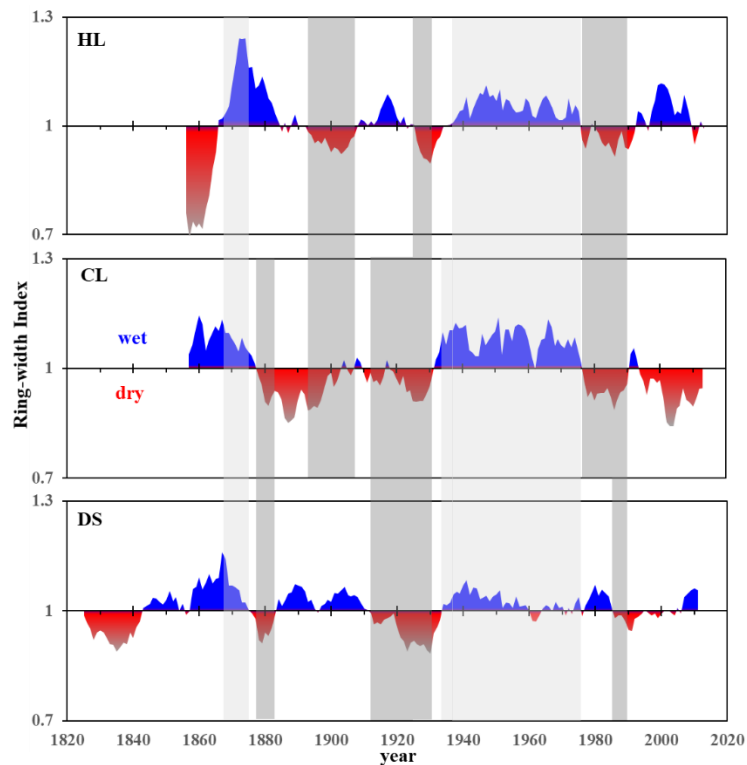
379

380 3.3.2 Characteristics of regional climate change at inter-decadal scales

381 On the decadal scale, the 11a running mean series indicates that at the HL site there
382 were four wetter periods (mid-1860s to early 1880s; 1910s to 1920s; mid-1930s to mid-
383 1970s; and late 1990s to early 2010s). Four drought periods were seen (mid-1850s to
384 mid-1860s; early 1890s to late 1900s; circa 1930s; and mid-1970s to 1980s) (Fig.5).



385



386

387 Figure 5. Three regional chronologies demonstrating alternation between dry (red) and
 388 wet (blue) years on interdecadal scales (11 a running mean). The gray and light gray
 389 bands indicate consistent changes of the dry and wet periods.

390 The CL regional chronology revealed two main wetter periods (mid-1850s to mid-
 391 1870s; mid-1930s to mid-1970s) and two longer drought periods (late 1870s to early
 392 1930s; following the late 1970s) (Fig.5).

393 The DS regional chronology showed four main wetter periods (mid-1840s to mid-
 394 1870s; mid-1880s to late 1900s; mid-1930s to mid-1980s; and late 2000s to early
 395 2010s). There were four drought periods (mid-1820s to mid-1840s; mid-1870s to 1880s;
 396 early 1910s to early 1930s; and late 1980s to mid-2000s). The drought during the last
 397 drought period was less severe (Fig.5).

398 The three chronologies show both synchronized phases and differential changes on
 399 an interdecadal scale. The more synchronized dry phases of climate change were the
 400 drought periods of the 1930s and 1990s. When we compared the DS chronology to the
 401 HL and CL chronologies on decadal scales, we noted that DS droughts tended to last
 402 longer and that they started and ended later than CL droughts. However, HL and DS
 403 droughts tended to end at ~~close to~~ the same time (Fig.5).

404 There were two wet periods in 1870s and the mid-1930s to 1970s which were
405 shared by all three sample sites. The latter period was the longest lasting wet period we
406 saw in our study. There were also dry and wet periods that were not shared by any of
407 our sites. There was an HL drought (mid-1850s to mid-1860s) which was not shared by
408 the other two sites, which were wetter. HL and CL shared drought periods (1890s to
409 1910s; 1980s) while DS was wetter. Conversely wetter periods at HL were sometimes
410 accompanied by drought in the other two sites. Drought at CL was sometimes
411 accompanied by wet periods at the other two sites. DS was wet during the 2010s but
412 the other two sites were in drought (Fig.5).

413 The results of the above studies show that there are diversified and complex
414 features in the interdecadal processes of climate change in different regions around the
415 Alxa Plateau.

416

417 **3.4 Driving mechanism of the regional climate changes**

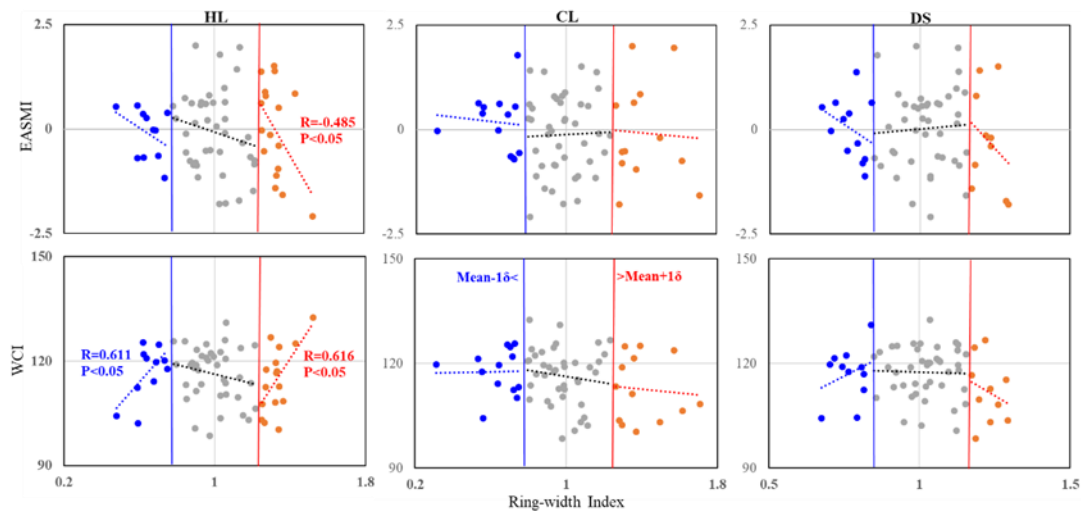
418 **3.4.1 Driving mechanism of the regional climate changes of typical years**

419 On the interannual scales, three regional chronologies we developed showed fairly
420 weak negative correlations between the EASM and the westerlies; none of the
421 correlations were statistically significant. We carried out correlation analyses of the
422 three regional ring-width chronologies and two major circulation indices. This was
423 done in high, medium and low ring-width index groups (Fig. 6; 7).

424 At HL, the results of our combined subgroup correlation analyses suggest that
425 correlations between radial growth groups and atmospheric circulations were stable.
426 Correlation between the higher ring-width group and atmosphere circulation indices
427 and between the lower ring-width group and the WCI were all significant ($P < 0.05$)
428 (Fig. 6; 7).

429 At CL, correlations between the higher and middle ring-width groups to the WCI
430 and the higher and middle WCI groups to the ring-width index were all negative.
431 Correlations between the higher and middle ring-width groups and the EASMI, and
432 between the higher and middle EASMI groups with the ring-width index were
433 inconsistent (Fig. 6; 7).

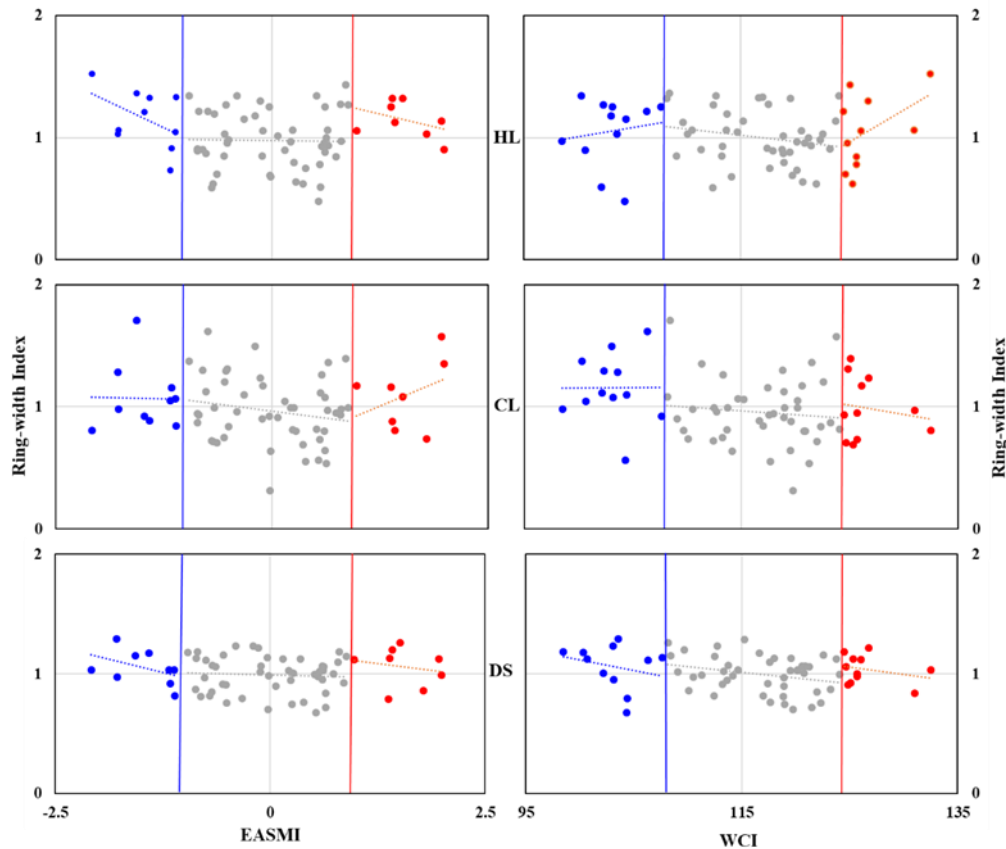
434 At DS, correlations between the higher and lower ring-width groups and the
 435 EASMI, and between the higher and lower EASMI groups to the ring-width indices,
 436 were consistent. The correlations between the higher ring-width groups and the WCI,
 437 and between the higher WCI groups and the ring-width index were consistent. However,
 438 the correlations between the lower ring-width groups and the WCI, also between the
 439 lower WCI groups and the ring-width index, were inconsistent (Fig. 6; 7).



440

441 Figure 6. Grouping related charts among the ring-width index of three regions (HL,
 442 CL and DS) and the two atmospheric circulations' indices (EASMI and WCI),
 443 grouped by chronological values. The noted numbers are the person correlation
 444 coefficients (two-tails test) and the corresponding significant credible level. Only the
 445 significant correlations were labeled. Red dots indicate the higher ring-width index
 446 group ($> \text{mean}+1\delta$), gray dots indicate the middle ring-width index group ($> \text{mean}-1\delta$
 447 $\sim < \text{mean}+1\delta$), and blue dots indicate the lower ring-width index group ($> \text{mean}-1\delta$).

448 Except for HL, none of the ring-width groups or the atmospheric circulation index
 449 groups of the others reached a level of significance. These results suggest that HL is
 450 strongly affected by size of, and the interaction between, the EASM and the
 451 westerlies-Westerly winds. On an interannual scale, stronger west winds and a weaker
 452 monsoon could result in variations from the ordinary climate (veering towards drier or
 453 wetter). Weaker west winds and a stronger monsoon formed the normal climate at HL.
 454 At the CL and DS sites, both atmospheric circulations were relatively weak on
 455 interannual scales. They had complex interactions.



456

457 Figure 7. Grouping related charts among the two atmosphere circulations' index
 458 (EASMI and WCI) and the ring-width index of three regions (HL, CL, and DS),
 459 grouped by the two atmosphere circulations' index. Red dots indicate the higher
 460 atmosphere circulations' index group ($> \text{mean}+1\delta$), gray dots indicate the middle
 461 atmosphere circulations' index group ($> \text{mean}-1\delta \sim < \text{mean}+1\delta$), and blue dots indicate
 462 the lower atmosphere circulations' index group ($> \text{mean}-1\delta$).

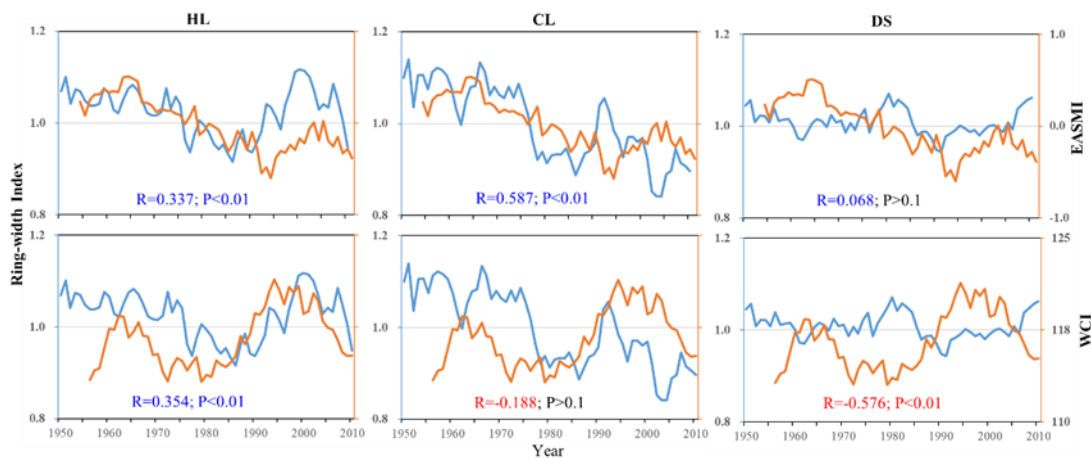
463

464 3.4.2 Driving mechanisms of the regional climate changes on a decadal scale

465 At HL, both the EASM and the westerly circulation had highly significant effects on
 466 the radial growth of the Qinghai spruce. At CL, the EASM also had highly significant
 467 effects on radial growth of the Qinghai spruce. There, correlation coefficients were
 468 higher for the EASMI (EASM index) than they were for the HL index. Correlations
 469 between the WCI and radial growth were negative, but not at a significant level.

470 At DS, correlation between radial growth and the WCI was extremely negative ($P <$
 471 ≤ 0.01). Correlation between radial growth and the EASM was positive ($P \geq 0.1$) (Fig.
 472 8). These results suggest that at HL, alternations between dry and wet seasons were

473 affected both by the EASM and the westerlies. If either of the two atmospheric
 474 circulations was stronger, the climate tended to be wetter. At CL, alternations between
 475 dry and wet were affected mainly by the EASM. When the EASM was stronger, the
 476 climate was wetter. At DS, the climate was affected mainly by the ~~westerly~~
 477 ~~winds.westerlies~~. The stronger the winds, the wetter the climate (Fig. 8).



478

479 Figure 8. Interdecadal scale (11-a running average) correlations of the three residual
 480 chronologies with the EASMI and WCI.

481 The results of our interdecadal partial correlation analysis of the three RES-
 482 chronologies with the WCI and EASMI further illustrate the impacts of the two
 483 circulation systems on the climate of the three regions (Table 32).

484 At HL, if we control one ~~factorvariable~~ (the WCI or EASMI) from our analysis,
 485 the other ~~factorvariable will all~~ showed a positive correlation (~~P<with its chronology (P~~
 486 ~~≤ 0.0001)~~). At CL, if we controlled the WCI, we find a positive significant correction
 487 ~~with-between the chronology and~~ EASMI (~~P< < 0.0001)~~). If we controlled the effect of
 488 EASMI, we saw a weak negative correction ~~withbetween the chronology and~~ WCI
 489 (Table 32). At DS, if we controlled EASMI, we saw a negative significant correlation
 490 ~~withbetween the chronology and~~ WCI (~~P< ≤ 0.0001)~~). If we controlled the WCI, we saw
 491 an insignificant negative correlation ~~withbetween the chronology and~~ EASMI (Table
 492 32).

493

Table 32. Inter-decadal partial correlation analysis of the three residual-chronologies with the WCI and EASMI.

	HL	CL	DS
WCI	0.489 ***	0.550***	-0.172
EASMI	0.511***	-0.001	-0.591***

Correlation significance levels (two-tailed test): *** P < 0.001.

Summary: at HL (on the eastern boundary of the Alxa Plateau), both EASMI and WCI influenced the alternation between wet and dry; at CL (on the southern boundary of the Alxa Plateau), climate was mainly influenced by the EASM. At DS (on the western boundary of the Alxa Plateau and the middle part of Hexi Corridor), climate was mainly influenced by the ~~westerly winds~~westerlies.

4. Discussion and conclusions

4.1 Climate changes indicated by regional chronologies

Our chronology-climate response analysis (Fig. 4) showed that the radial growth index of Qinghai spruce in the HL, CL and DS mountains were a good record of regional climate changes around the Alxa Plateau (Fig. 3). On the interannual scale, the three regional chronologies noted that the extreme drought years of 1928, 1957 and 1981 were shared by two or more locations, as were the drought years of 1854, 1861, 1916, 1926, 1947, 1966, and 2001 (Fig. 3 and Table-3).

We note that drought was also reported by other tree-ring studies for these regions (Chen et al., 2016), also for the Qilian Mountains (Zhang et al., 2011; Zhang et al., 2017). Several other drought years (1854, 1884, and 1925–1928) were also seen in the dry-wet climate history (PDSI) ~~(and~~ recorded by tree-ring-widths) in the nearby area of Mount Hasi, which lies on the edge of the regions most influenced by the EASM (Kang et al., 2012).

The drought years of 1823, 1833, 1854, 1877, 1883–1885, 1895, 1908, 1971, 1992, and 2003 seen in results for the Alxa Plateau are also seen in twelve tree-ring reconstructed drought series for the Qilian Mountains (an area mainly influenced by ~~westerly winds~~westerlies) (Zhang et al., 2011). We also note that wetter years seen in

521 our three regional chronologies were also seen in results from the Hasi and Xinglong
522 Mountains, which are also on the edge of the area influenced by the EASM) (Fang et
523 al., 2009; Kang et al., 2012).

524 If we compare our results with those seen for the EASM-affected areas at Mount
525 Guiqing, 1820–2005 (Fang et al., 2010), we noted that only three of the eight drought
526 years in that area (1928, 2000, and 2001) were seen in our three chronologies. We also
527 noted results from the westerly-influenced area at Mount Tianshan (Jiang et al., 2017).
528 The wetter years of 1846, 1903 and 1942 at DS were also extreme wet years at Mount
529 Tianshan. Two wet years, 1848 and 1959, recorded at DS are either one year earlier or
530 one year later than extremely wet years at Mount Tianshan, which might suggest some
531 correlation. Drier years at DS (1884, 1947 and 1951) are one or two years later than the
532 extremely dry years at Mount Tianshan. This suggests that these phenomena could be
533 related to broader changes in the extent and strength of the atmospheric circulation.

534 On a broader (interdecadal) scale, an extreme drought period in 1920s–1930s was
535 shared by much of northern China (Liang et al., 2006; Fang et al., 2009; Fang et al.,
536 2010). This is the same drought that we note our chronologies for HL, CL and DS (Liu
537 et al., 2002; Chen et al., 2010; Fan et al., 2012; Liu et al., 2013; Zhang et al., 2015). A
538 drought in 1890–1900 was noted by dendrochronological studies and regional history
539 documents (Yuan, 1994; Ma et al., 2003; Cai and Liu, 2007).

540 Ma and Fu's (2006) study showed a broad shift towards a drying climate in 1977–
541 78 (eastern area in northwestern China, also northern China). Several other
542 dendrochronological studies showed a combination of high temperatures and low
543 precipitation in the late 1970s to early 1990s (Zhang et al., 2005b; Cai and Liu, 2007;
544 Cai, 2009).

545 This same drought was seen at DS, if somewhat later and for a shorter time. We
546 also noted its effects at HL and CL. This would be consistent with the increased
547 humidity of the climate in the eastern region of Northwest China (the EASM-influenced
548 region experiencing >400 mm precipitation). This region would include Mount
549 Xinglong (Fang et al., 2009; Chen et al. 2015), the easternmost part of the Qilian
550 Mountains, and Mount Guiqing (Fang et al., 2010).

551 The wet period that lasted from the 1940s to the early 1970s has been recorded by
552 several tree-ring-width chronologies covering HL, CL, and DS (Liu et al., 2004; Liu et
553 al., 2005; Gao et al., 2006; Cai, 2009; Chen et al., 2010). Regional history documents
554 also record some severe floods disasters in this period (Yuan, 1994). We also see this
555 wet period in tree-ring-width chronologies from Mount Xinglong (Fang et al., 2009;
556 Chen et al. 2015) and Mount Guiqing (Fang et al., 2010).

557 The wet period in the 1830s–1840s evident in the chronologies in Xinglong
558 Mountain (Fang et al., 2009)(Chen et al. 2015) and Guiqing Mountain (Fang et al.,
559 2010) corresponds to the dry period of DS. The wet period in the 1830s–1840s
560 corresponds to the dry period of HL and CL, and to the wet period of DS. The observed
561 phenomena can be attributed to differences in the extent and intensity of EASM and
562 westerly atmospheric circulations.

563

564 **4.2 Influence of atmospheric circulations and their interaction on climate change** 565 **in the Alxa Plateau**

566 ~~It is known that that water~~Water vapor carried by the ~~westerly winds~~westerlies will
567 extend southward to the northern part of Qinghai, the Hexi region of Gansu, the
568 northern part of Ningxia, and the northern part of Shaanxi Province, sometimes passing
569 through the northern border of the Xinjiang region (Li et al., 2012). The area bounded
570 by 35° and 55°N, and 110°E and 140°E seems to keybe crucial to fluctuations in the
571 ~~westerly winds~~westerlies. This in turn affects the distribution of rain belts in summer.
572 Its mean WCI are weaker positively to the rainfall in the middle of Yellow River Basin
573 and its northern regions (Yan et al., 2007)~~).~~. The results showed that the middle ring-
574 width index group of Qinghai spruce in the three sample sites, which are located in the
575 key area for interaction between wind and monsoon, presented weaker negative
576 correlation with WCI on the interannual scale (Fig. 6).

577 The EASM boundary zone has a greater influence on precipitation at higher
578 latitudes and thus on vegetation growth. This boundary zone can fluctuate due to the
579 interannual variability of the EASM and the westerlies. There may be lagging effects
580 at the mid-latitudes (Ou and Qian, 2006). Again, we note that on an interannual scale,

581 there is much variation in the strengths and interactions of the EASM and westerly
582 circulation and thus on climate in our three study regions (Fig. 6).

583 Sun et al. (2019) showed that when the westerly circulation strengthens, high
584 latitude air pressure drops across the entire Asian continent. Siberian high pressures and
585 the EASM are weakened. The south of the cold air activity is also correspondingly
586 weakened. That is not conducive to the north and south of the cold and warm air vapor
587 exchange to form precipitation. When the lower of the WCI and weakened latitudinal
588 circulation, the meridional circulation will strengthen, which favors the exchange of
589 warm and cold air between the north and south to form precipitation.

590 Yang et al. (2019) proposed that in years with weak summer westerlies in the
591 middle latitudes, the upper-level jet stream tends to shift southward. This southward
592 displacement of the jet stream, coupled with weakened lower-level divergence, hampers
593 the northward transport of warm air into the southwestern region. Consequently, this
594 leads to reduced availability of water vapor sources and ultimately results in diminished
595 summer precipitation within the transitional zone of typical monsoon activity. If the jet
596 stream moves northward, precipitation increases.

597 Xu et al. (2010) wrote that in the middle Qilian Mountains the ~~westerly~~
598 ~~winds~~westerlies affect precipitation directly, while the EASM only indirectly affects
599 precipitation. When the ~~westerly~~~~winds~~westerlies are stronger, the high precipitation
600 zone moves northwestward; when they are weaker, the zone moves southeastward.

601 At DS, radial growth showed weak negative correlations with higher WCI and also
602 higher, middle, and lower EASMI groups (Figs. 6;_7). At HL, when high chronology
603 indices are positive they are significantly correlated with westerly circulation; when
604 they are negative they significantly correlate with EASM (Figs. 6; 7). At CL, which lies
605 further to the south than HL, a higher EASMI leads to a more humid climate. Other
606 effects are more complicated: for example, the higher and lower ring-width index
607 groups, associated with extreme dry and wet climate years, have weak negative
608 correlations to EASMI (Figs. 6; 7). Jiang et al. (2019) published the results of their
609 hydrogen and oxygen isotope studies of surface water at more than 3,000 sampling sites
610 in northern China. They showed that surface water recharge in the DS Mountains is due

611 to the ~~westerly winds~~westerlies; recharge in the CL Mountains is due to the EASM. The
612 HL Mountains, in contrast, sit at the boundary of the EASM; water recharge there is
613 due to both the EASM and the westerlies.

614 Jiang and Wang (2005) notes significant declines in the EASM in the mid-1960s
615 and mid-1970s, which led to decline in the radial growth of Qinghai spruce in our study
616 area. The effect of the latter declined period was much greater than that of the former,
617 whatever the intensity or duration. The effects of these declines were stronger at CL
618 and DS than at HL. In the mid-1970s, EASM retreat had stronger negative effects at
619 CL and then at HL. However, decline in the EASM proved to be a facilitator of radial
620 growth at DS (Fig. 8).

621 In the same period the westerly circulation also retreated. The EASM retreated
622 again in 1990s, while the ~~westerly winds~~westerlies strengthened. This resulted in a drier
623 climate in the CL Mountains. However, it was also correlated with fluctuating wet
624 periods at HL and a weak wet period at DS. The above results, to a certain extent,
625 support our view on the driving mechanisms of climate change in the three study areas,
626 especially in the DS Mountains.

627 When we look at this area on a geologic scale, we learn that the westerly circulation
628 strengthened during the Ice Age. Westerly jet streams moved southward to about 35°N.
629 When the ~~westerly winds~~westerlies weakened in the Interglacial Age, the westerly jet
630 streams moved northward to ~37°N (Sun et al., 2003). A study of Holocene lake level
631 evolution in the ancient Zhuye lake, central Alxa Plateau, showed that lake-level change
632 was subject to the combined effects of EASM and the arid climate of Central Asia (Li,
633 2009) This result further illustrates the complexity of lake evolution and climate change
634 in the EASM marginal zone.

635 The westerly circulation also interacts with the monsoon on the Tibetan Plateau,
636 which has a profound effect on the climate of the Asian monsoon region as well as the
637 global climate (Qu et al., 2004). There has also been much research using proxy
638 indicator cycles indicating that our study area is also influenced by large-scale climate
639 and ocean-atmosphere changes on interannual and interdecadal scales, such as the
640 North Atlantic Oscillation (NAO), Pacific Decadal Oscillation (PDO), El Niño-

641 Southern Oscillation (ENSO), and sunspot activity (Gou et al., 2015a; 2015b; Liu et al.,
642 2016; Wang et al., 2017).

643 However, all of the above-mentioned large-scale climate and ocean-atmosphere
644 changes affect the EASM and westerly circulation through different pathways (Li,
645 2009), which in turn have various effects on the northwestern edge zone of the EASM
646 and the zone of interaction between the two major atmospheric circulations.

647 In conclusion, based on the analysis of the regional chronologies collected in the
648 HL, CL and DS mountains that are arrayed around the Alxa Plateau, we can safely assert
649 that the radial growth of Qinghai spruce in the study area is mainly affected by regional
650 precipitation. This precipitation varies constantly over time and space, primarily
651 influenced by the interactions between two atmospheric circulation systems, EASM
652 and ~~westerly winds~~westerlies. At HL, both of these atmospheric circulation systems
653 play a significant role in shaping climate changes. At CL, the climate is mainly
654 influenced by the EASM. At DS, climate is more heavily influenced by the westerly
655 circulation.

656 In the future, it is to be hoped that more refined, smaller scale research can be done
657 on the climate history in the deserts of the Alxa Plateau. Such research may finally to
658 provide a theoretical basis to explain –regional climate driving mechanisms and thus
659 enable better desertification controls.

660

661 ~~Competing interests: The contact author has declared that none of the authors has any~~
662 ~~competing interests.~~

663

664 **Acknowledgements**

665 The study was jointly funded by the National Natural Science Foundation of China
666 (NSFC) (No.42171031; 42171167); Inner Mongolia Autonomous Region Special Fund
667 project for transformation of Scientific and technological Achievements (2021CG0046).

668

669 **References**

- 670 Cai, Q. F.: Response of *Pinus tabulaeformis* tree-ring growth to three moisture indices and
671 January to July Walter index reconstruction in Helan mountain, Marine geology &
672 Quaternary geology, 29, 131–136 (In Chinese with English abstract),
673 <https://doi.org/10.3724/SP.J.1140.2009.06131>, 2009.
- 674 Cai, Q. F. and Liu, Y.: January to August temperature variability since 1776 inferred from tree-
675 ring width of *Pinus tabulaeformis* in Helan Mountain, Journal of Geographical Sciences,
676 17, 293–303, <https://doi.org/10.1007/s11442-007-0293-5>, 2007.
- 677 Chen, F., Yuan, Y. J., Zhang, T. W., and Linderholm, H. W.: Annual precipitation variation for
678 the southern edge of the Gobi Desert (China) inferred from tree rings: linkages to climatic
679 warming of twentieth century, Nat. Hazards, 81, 939–955, [https://doi.org/10.1007/s11069-](https://doi.org/10.1007/s11069-015-2113-z)
680 015-2113-z, 2016.
- 681 Chen, F., Wei, W. S., Yuan, Y. J., Yu, S. L., Shang, H. M., Zhang, T. W., Zhang, R. B., Wang, H.
682 Q., and Qin, L.: Variation of annual precipitation during 1768–2006 in Gansu Inferred from
683 multi-site tree-ring chronologies, Journal of Desert Research, 33, 1520–1526 (In Chinese
684 with English abstract), <https://doi.org/10.7522/j.issn.1000-694X.2013.00218.>, 2013.
- 685 Chen, F., Yuan, Y. J., Wei, W. S., Yu, S. L., Fan, Z. A., Zhang, R. B., Zhang, T. W., Li, Q., and
686 Shang, H. M.: Temperature reconstruction from tree-ring maximum latewood density of
687 Qinghai spruce in middle Hexi Corridor, China, Theoretical and Applied Climatology, 107,
688 633–643, <https://doi.org/10.1007/s00704-011-0512-y>, 2012.
- 689 Chen, F., Yuan, Y. J., Wei, W. S., Yu, S. L., Li, Y., Zhang, R., Fan, Z., Zhang, T., and Shang, H.:
690 PDSI changes of May to July recorded by tree rings in the northern Helan Mountains,
691 Advance in Climate Changes Research, 65, 344–348 (In Chinese with English abstract),
692 2010.
- 693 Chen, F. H., Chen, J. H., Huang, W., Chen, S. Q., Huang, X. Z., Jin, L. Y., Jia, J., Zhang, X. J.,
694 An, C., and Zhang, J.: Westerlies Asia and monsoonal Asia: spatiotemporal differences in
695 climate change and possible mechanisms on decadal to sub-orbital timescales, Earth-Sci.
696 Rev., 192, 337–354, <https://doi.org/10.1016/j.earscirev.2019.03.005>, 2019a.
- 697 Chen, F. H., Fu, B. J., Xia, J., Wu, D., Wu, S. H., Zhang, Y. L., Sun, H., Liu, Y., Fang, X. M.,
698 Qin, B. Q., Li, X., Zhang, T. J., Liu, B. Y., Dong, Z. B., Hou, S. G., Tian, L. D., Xu, B. Q.,
699 Dong, G. H., Zheng, J. Y., Yang, W., Wang, X., Li, Z. J., Wang, F., Hu, Z. B., Wang, J.,
700 Liu, J. B., Chen, J. H., Huang, W., Hou, J. Z., Cai, Q. F., Long, H., Jiang, M., Hu, Y. X.,
701 Feng, X. M., Mo, X. G., Yang, X. Y., Zhang, D. J., Wang, X. H., Yin, Y. H., and Liu, X.
702 C.: Major advances in studies of the physical geography and living environment of China
703 during the past 70 years and future prospects, Science China Earth Sciences, 62, 1665–
704 1701, <https://doi.org/10.1007/s11430-019-9522-7>, 2019b.
- 705 Chen, J., Huang, W., Jin, L., Chen, J. H., Chen, S. Q., and Chen, F. H.: A climatological northern
706 boundary index for the East Asian summer monsoon and its interannual variability,
707 Science China Earth Sciences, 61, 13–22, <https://doi.org/10.1007/s11430-017-9122-x>,
708 2018.
- 709 [Cook E.R.: A Time Series Analysis approach to tree ring standardization \(Dendrochronology.](#)

- 710 [forestry, dendroclimatology, autoregressive process\)\[D\]. Tuscon, Arizona: The University](#)
711 [of Arizona, 1985.](#)
- 712 Ding, Y. H., Liu, Y. J., Xu, Y., Wu, P., Xue, T., Wang, J., Shi, Y., Zhang, Y. X., Song, Y. F., and
713 Wang, P. L.: Regional responses to global climate change: progress and prospects for trend,
714 causes, and projection of climatic warming-wetting in Northwest China, *Advances in*
715 *Earth Science*, 38, 551–562 (In Chinese with English abstract),
716 <https://doi.org/10.11867/j.issn.1001-8166.2023.027>, 2023.
- 717 Fan, Z. A., Wei, W. S., Chen, F., and Yuan, Y. J.: Precipitation variation from 1775 to 2005 at
718 the eastern margin of Tengger Desert, China inferred from tree-ring, *Journal of Desert*
719 *Research*, 32, 996–1002 (In Chinese with English abstract), 2012.
- 720 Fang, K. Y., Gou, X. H., Chen, F. H., D'arrigo, R., and Li, J. B.: Tree-ring based drought
721 reconstruction for the Guiqing Mountain (China): linkages to the Indian and Pacific
722 Oceans, *Int. J. Climatol.*, 30, 1137–1145, <https://doi.org/10.1002/joc.1974>, 2010.
- 723 Fang, K. Y., Gou, X. H., Chen, F. H., Yang, M. X., Li, J. B., He, M. S., Zhang, Y., Tian, Q. H.,
724 and Peng, J. F.: Drought variations in the eastern part of northwest China over the past two
725 centuries: evidence from tree rings, *Clim. Res.*, 38, 129–135,
726 <https://doi.org/10.3354/cr00781>, 2009.
- 727 Feng, W., Wang, K. L., and Jiang, H.: Influences of westerly wind inter-annual change on water
728 vapor transport over northwest china summer, *Plateau Meteorology*, 23, 270–275 (In
729 Chinese with English abstract), 2004.
- 730 Gao, S. Y., Lu, R. J., Qiang, M. R., Ha, S., Zhang, D. S., Chen, Y., and Xia, H.: Precipitation
731 variation recorded by tree-rings in the northern Tengger Desert of the last 140 years, *Chin.*
732 *Sci. Bull.*, 51, 326–331, <https://doi.org/10.1360/csb2006-51-3-326>, 2006.
- 733 Gou, X. H., Gao, L. L., Deng, Y., Chen, F. H., Yang, M. X., and Still, C.: An 850 - year tree -
734 ring - based reconstruction of drought history in the western Qilian Mountains of
735 northwestern China, *Int. J. Climatol.*, 35, 3308–3319, <https://doi.org/10.1002/joc.4208>,
736 2015a.
- 737 Gou, X. H., Deng, Y., Gao, L. L., Chen, F. H., Cook, E., Yang, M. M., and Zhang, F.: Millennium
738 tree-ring reconstruction of drought variability in the eastern Qilian Mountains, northwest
739 China, *Climate Dynamics*, 45, 1761–1770, <https://doi.org/10.1007/s00382-014-2431-y>,
740 2015b.
- 741 Huang, L. X., Chen, J., Yang, K., Yang, Y. J., Huang, W., Zhang, X., and Chen, F. H.: The
742 northern boundary of the Asian summer monsoon and division of westerlies and monsoon
743 regimes over the Tibetan Plateau in present-day, *Science China Earth Sciences*, 66, 882–
744 893, <https://doi.org/10.1007/s11430-022-1086-1>, 2023.
- 745 Jiang, D. B. and Wang, H. J.: Natural interdecadal weakening of East Asian summer monsoon
746 in the late 20th century, *Chin. Sci. Bull.*, 50, 1923–1929, [https://doi.org/10.1360/982005-](https://doi.org/10.1360/982005-36)
747 36, 2005.
- 748 Jiang, P., Liu, H. Y., Wu, X. C., and Wang, H. Y.: Tree-ring-based SPEI reconstruction in central

- 749 Tianshan Mountains of China since A.D. 1820 and links to westerly circulation, *Int. J.*
750 *Climatol.*, 37, 2863–2872, <https://doi.org/10.1002/joc.4884>, 2017.
- 751 Jiang, W. J., Wang, G. C., Sheng, Y. Z., Shi, Z. M., and Zhang, H.: Isotopes in groundwater (^2H ,
752 ^{18}O , ^{14}C) revealed the climate and groundwater recharge in the Northern China, *Sci. Total*
753 *Environ.*, 666, 298–307, <https://doi.org/10.1016/j.scitotenv.2019.02.245>, 2019.
- 754 Kang, S. Y. and Yang, B.: Precipitation variability at the northern fringe of the Asian summer
755 monsoon in Northern China and its possible mechanism over the past 530 years,
756 *Quaternary Sciences*, 35, 1185–1193, [https://doi.org/10.11928/j.issn.1001-](https://doi.org/10.11928/j.issn.1001-7410.2015.05.14)
757 7410.2015.05.14, 2015.
- 758 Kang, S. Y., Yang, B., and Qin, C.: Recent tree-growth reduction in north central China as a
759 combined result of a weakened monsoon and atmospheric oscillations, *Clim. Change*, 115,
760 519–536, <https://doi.org/10.1007/s10584-012-0440-6>, 2012.
- 761 Li, D. L., Shao, P. C., and Wang, H.: The position variations of the north boundary of East Asia
762 subtropical summer monsoon in 1951–2009, *Journal of Desert Research*, 33, 1511–1519
763 (In Chinese with English abstract), <https://doi.org/10.7522/j.issn.1000-694X.2013.00217>,
764 2013.
- 765 Li, J. L., Li, Z. R., Yang, J. C., Shi, Y. Z., and Fu, J.: Analyses on spatial distribution and
766 temporal variation of atmosphere water vapor over northwest China in summer of later 10
767 years, *Plateau Meteorology*, 31, 1574–1581 (In Chinese with English abstract), 2012.
- 768 Li, J. P. and Zeng, Q. C.: A new monsoon index, its interannual variability and related with
769 monsoon precipitation, *Climatic and Environmental Research*, 10, 351–365 (In Chinese
770 with English abstract), 2005.
- 771 Li, W. L., Wang, K. L., Fu, S. M., and Jiang, H.: The interrelationship between regional Westerly
772 index and the water vapor budget in Northwest China, *Journal of Glaciology and*
773 *Geocryology*, 30, 28–34 (In Chinese with English abstract), 2008.
- 774 Li, Y.: The pollen records from lake sediments and climate & lake model in the Marginal area
775 of Asian monsoon, Lanzhou University, Lanzhou, China, 2009.
- 776 Li, Z. X., Feng, Q., Song, Y., Wang, Q. J., Yang, J., Li, Y. G., Li, J. G., and Guo, X. Y.: Stable
777 isotope composition of precipitation in the south and north slopes of Wushaoling Mountain,
778 northwestern China, *Atmospheric Research*, 182, 87–101,
779 <https://doi.org/10.1016/j.atmosres.2016.07.023>, 2016.
- 780 Liang, E. Y., Liu, X. H., Yuan, Y. J., Qin, N. S., Fang, X. Q., Huang, L., Zhu, H. F., Wang, L.,
781 and Shao, X. M.: The 1920s drought recorded by tree rings and historical documents in
782 the semi-arid and arid areas of Northern China, *Clim. Change*, 79, 403–432,
783 <https://doi.org/10.1007/s10584-006-9082-x>, 2006.
- 784 Liu, J. B., Chen, J., Chen, S. Q., Yan, X. W., Dong, H. R., and Chen, F. H.: Dust storms in
785 northern China and their significance for the concept of the Anthropocene, *Science China*
786 *Earth Sciences*, 65, 921–933, <https://doi.org/10.1007/s11430-021-9889-8>, 2022.

- 787 Liu, Y., Cai, Q. F., Ma, L. M., and An, Z. S.: Tree ring precipitation records from Baotou and
788 the East Asia summer monsoon variations for the last 254 years, *Earth Sci. Front.*, 8, 91–
789 97 (In Chinese with English abstract), <https://doi.org/10.3321/j.issn:1005-2321.2001.01.012>, 2001.
- 791 Liu, Y., Sun, C. F., Li, Q., and Cai, Q. F.: A *Picea crassifolia* tree-ring width-based temperature
792 reconstruction for the Mt. Dongda region, Northwest China, and its relationship to large-
793 scale climate forcing, *PLoS One*, 11, e0160963,
794 <https://doi.org/10.1371/journal.pone.0160963>, 2016.
- 795 Liu, Y., Lei, Y., Sun, B., Song, H. M., and Li, Q.: Annual precipitation variability inferred from
796 tree-ring width chronologies in the Changling–Shoulu region, China, during AD 1853–
797 2007, *Dendrochronologia*, 31, 290–296, <https://doi.org/10.1016/j.dendro.2013.02.001>,
798 2013.
- 799 Liu, Y., Won-Kyu, P., Cai, Q. F., Jung-Wook, S., and Hyun-Sook, J.: Monsoonal precipitation
800 variation in the East Asia since A.D. 1840—tree-ring evidences from China and Korea,
801 *Science in China Series D: Earth Sciences*, 46, 1031–1039,
802 <https://doi.org/10.1007/BF02959398>, 2003.
- 803 Liu, Y., Ma, L. M., Cai, Q. F., An, Z. S., Liu, W. G., and Gao, L. Y.: Reconstruction of summer
804 temperature (June–August) at Mt. Helan, China, from tree-ring stable carbon isotope
805 values since AD 1890, *Science in China Series D: Earth Sciences*, 45, 1127–1136,
806 <https://doi.org/10.1360/02yd9109>, 2002.
- 807 Liu, Y., Cai, Q. F., Liu, W. G., Yang, Y. K., Sun, J. Y., Song, H. M., and Li, X. X.: Monsoon
808 precipitation variation recorded by tree-ring $\delta^{18}\text{O}$ in arid Northwest China since AD 1878,
809 *Chemical Geology*, 252, 56–61, <https://doi.org/10.1016/j.chemgeo.2008.01.024>, 2008.
- 810 Liu, Y., Cai, Q. F., Shi, J. F., Hughes, M. K., Kutzbach, J. E., Liu, Z. Y., Ni, F. B., and An, Z. S.:
811 Seasonal precipitation in the south-central Helan Mountain region, China, reconstructed
812 from tree-ring width for the past 224 years, *Canadian Journal of Forest Research*, 35,
813 2403–2412, <https://doi.org/10.1139/x05-168>, 2005.
- 814 Liu, Y., Shi, J. F., Shishov, V., Vaganov, E., Yang, Y. K., Cai, Q. F., Sun, J. Y., Wang, L., and
815 Djanseitov, I.: Reconstruction of May–July precipitation in the north Helan Mountain,
816 Inner Mongolia since A.D. 1726 from tree-ring late-wood widths, *Chin. Sci. Bull.*, 49,
817 405–409, <https://doi.org/10.1007/BF02900325>, 2004.
- 818 Ma, L. M., Liu, Y., Cai, Q. F., and An, Z. S.: The precipitation records from tree-ring late wood
819 width in the helan mountain, *Marine geology & Quaternary geology*, 23, 109–114 (In
820 Chinese with English abstract), <https://doi.org/10.16562/j.cnki.0256-1492.2003.04.016>,
821 2003.
- 822 Ma, M. J., Pu, Z. X., Wang, S. G., and Zhang, Q. A.: Characteristics and numerical simulations
823 of extremely large atmospheric boundary-layer heights over an arid region in north-west
824 china, *Boundary-Layer Meteorology*, 140, 163–176, <https://doi.org/10.1007/s10546-011-9608-2>,
825 2011.

- 826 Ma, Z. G. and Fu, C. B.: The basic facts of aridity in northern China from 1951 to 2004, Chin.
827 Sci. Bull., 51, 2429–2439 (In Chinese), <https://doi.org/10.1360/csb2006-51-20-2429>,
828 2006.
- 829 Ou, T. H. and Qian, W. H.: Vegetation variations along the monsoon boundary zone in East
830 Asia, Chinese Journal of Geophysics, 49, 698–705 (In Chinese with English abstract),
831 2006.
- 832 Qin, L., Liu, G. X., Li, X. Z., Chongyi, E., Li, J., Wu, C. R., Guan, X., and Wang, Y.: A 1000-
833 year hydroclimate record from the Asian summer monsoon-Westerlies transition zone in
834 the northeastern Qinghai-Tibetan Plateau, Clim. Change, 176, 1–20, [https://doi.org/](https://doi.org/10.1007/s10584-023-03497-1)
835 [/10.1007/s10584-023-03497-1](https://doi.org/10.1007/s10584-023-03497-1), 2023.
- 836 Qu, W. J., Zhang, X. H., Wang, D., Shen, Z. X., Mei, F. M., Cheng, Y., and Yan, L. W.: The
837 important significance of westerly wind study, Marine Geology and Quaternary Geology,
838 24, 125–132 (In Chinese with English abstract), [https://doi.org/10.16562/j.cnki.0256-](https://doi.org/10.16562/j.cnki.0256-1492.2004.01.018)
839 [1492.2004.01.018](https://doi.org/10.16562/j.cnki.0256-1492.2004.01.018), 2004.
- 840 Shao, X. M., Xu, Y., Yin, Z. Y., Liang, E. Y., Zhu, H. F., and Wang, S.: Climatic implications of
841 a 3585-year tree-ring width chronology from the northeastern Qinghai-Tibetan Plateau,
842 Quaternary Science Reviews, 29, 2111–2122,
843 <https://doi.org/10.1016/j.quascirev.2010.05.005>, 2010.
- 844 Sun, D. H., An, Z. S., Su, R. H., Deer, H. Y., and Sun, Y. B.: The dust deposition records of the
845 evaluation of Asia monsoon and Westerly circulation in north China in the last 2.6Ma,
846 Science in China (Series D), 33, 497–504 (In Chinese), 2003.
- 847 Sun, L. Q., Li, T. J., Li, Q. L., and Wu, Y. P.: Responses of autumn flood peak in the Yellow
848 River source regions to westerly circulation index, Journal of Glaciology and Geocryology,
849 41, 1475–1482 (In Chinese with English abstract), [https://doi.org/10.7522/j.issn.1000-](https://doi.org/10.7522/j.issn.1000-0240.2019.0028)
850 [0240.2019.0028](https://doi.org/10.7522/j.issn.1000-0240.2019.0028), 2019.
- 851 Tang, X., Qian, W. H., and Liang, P.: Climatic features of boundary belt for East Asian Summer
852 Monsoon, Plateau Meteorology, 25, 375–381 (In Chinese with English abstract), 2006.
- 853 [Vicente-Serrano, S.M., Beguería, S. and López-Moreno, J.I.: A multiscale drought index](https://doi.org/10.1175/2009jcli2909.1)
854 [sensitive to global warming: the standardized precipitation evapotranspiration index. J.](https://doi.org/10.1175/2009jcli2909.1)
855 [Clim., 23\(7\): 1696–1718, https://doi.org/10.1175/2009jcli2909.1., 2010.](https://doi.org/10.1175/2009jcli2909.1)
- 856 Wang, B. J., Huang, Y. X., He, J. H., and Wang, L. J.: Relation between vapour transportation
857 in the period of East Asian Summer Monsoon and drought in Northwest China, Plateau
858 Meteorology, 23, 912–917 (In Chinese with English abstract), 2004.
- 859 Wang, J. L., Yang, B., Ljungqvist, F. C., Luterbacher, J., Osborn, Timothy J., Briffa, K. R., and
860 Zorita, E.: Internal and external forcing of multidecadal Atlantic climate variability over
861 the past 1,200 years, Nature Geoscience, 10, 512–517, <https://doi.org/10.1038/ngeo2962>,
862 2017.
- 863 Wang, K. L., Jiang, H., and Zhao, H. Y.: Atmospheric water vapor transport from westerly and
864 monsoon over the Northwest China, Advances in Water Science, 16, 432–438 (In Chinese

- 865 with English abstract), <https://doi.org/10.14042/j.cnki.32.1309.2005.03.021>, 2005.
- 866 [Wigley, T.M.L., Briffa, K.R., Jones, P.D. On the average value of correlated time series, with](#)
867 [applications in dendroclimatology and hydrometeorology. Journal of Climate and Applied](#)
868 [Meteorology 23\(2\), 201–213, 1984.](#)
- 869 Xiao, S. C., Chen, X. H., and Ding, A. J.: Study process of climate changes, environment
870 evolution and its driving mechanism in the last two centuries in the Alxa Desert, Journal
871 of Desert Research, 37, 1102–1201 (In Chinese with English abstract),
872 [10.7522/j.issn.1000-694x.2017.00002](https://doi.org/10.7522/j.issn.1000-694x.2017.00002), 2017.
- 873 Xiao, S. C., Yan, C. Z., Tian, Y. Z., Si, J. H., Ding, A. J., Chen, X. H., Han, C., and Teng, Z. Y.:
874 Regionalization for desertification control and countermeasures in the Alxa Plateau, China,
875 Journal of Desert Research, 39, 182–192 (In Chinese with English abstract),
876 <https://doi.org/10.7522/j.issn.1000-694X.2019.00068>, 2019.
- 877 Xu, J. J., Wang, K. L., Jiang, H., Li, Z. G., Sun, J., Luo, X. P., and Zhu, Q. L.: A numerical
878 simulation of the effects of Westerly and Monsoon on precipitation in the Heihe River
879 Basin, Journal of Glaciology and Geocryology, 32, 489–496 (In Chinese with English
880 abstract), 2010.
- 881 Yan, H. S., Hu, J., Fan, K., and Zhang, Y. J.: The analysis of relationship between the variations
882 of Westerly Index in summer and precipitation during the flood period over China in the
883 last 50 years. , Chinese Journal of Atmospheric Science, 31, 717–726 (In Chinese with
884 English abstract), 2007.
- 885 Yang, B., Qin, C., Wang, J. L., He, M. H., Melvin, T. M., Osborn, T. J., and Briffa, K. R.: A
886 3,500-year tree-ring record of annual precipitation on the northeastern Tibetan Plateau,
887 Proc. Natl. Acad. Sci. USA, 111, 2903–2908, <https://doi.org/10.1073/pnas.1319238111>,
888 2014.
- 889 Yang, J. H., Zhang, Q., Liu, X. Y., Yue, P., Shang, J. L., Ling, H., and Li, W. J.: Spatial-temporal
890 characteristics and causes of summer precipitation anomalies in the transitional zone of
891 typical summer monsoon, China, Chinese Journal of Geophysics, 62, 4120–4128 (In
892 Chinese with English abstract), <https://doi.org/10.6038/cjg2019M0639>, 2019.
- 893 Yuan, L.: Hazards history in northwestern China, Gansu people's press, Lanzhou, China1994.
- 894 Zhang, F., Chen, Q. M., Su, J. J., Deng, Y., Gao, L. L., and Gou, X. H.: Tree-ring recorded of
895 the drought variability in the northwest monsoon marginal, China, Journal of Glaciology
896 and Geocryology, 39, 245–251 (In Chinese with English abstract),
897 <https://doi.org/10.7522/j.issn.1000-0240.2017.0028>, 2017.
- 898 Zhang, Q., Yang, J. H., Wang, P. L., Yu, H. P., Yue, P., Liu, X. Y., Lin, J. J., Duan, X. Y., Zhu,
899 B., and Yan, X. Y.: Progress and prospect on climate warming and humidification in
900 Northwest China, Chin. Sci. Bull., 68, 1814–1828, <https://doi.org/10.1360/TB-2022-0643>,
901 2023.
- 902 Zhang, Q. B., Cheng, G. D., Yao, T. D., Kang, X. C., and Huang, J. G.: A 2,326 year tree-ring
903 record of climate variability on the northeastern Qinghai-Tibetan Plateau, Geophys. Res.

- 904 Lett., 30, 1739, <https://doi.org/10.1029/2003GL017425>, 2003.
- 905 Zhang, Q. L., Liu, W. G., Liu, Y., Ning, Y. F., and Wen, Q. B.: Relationship between the stable
906 carbon and oxygen isotopic compositions of tree ring in the Mt. Helan region,
907 Northwestern China, *Geochimica*, 34, 51–56, <https://doi.org/10.19700/j.0379-1726.2005.01.006>, 2005a.
- 909 Zhang, S., Xu, H., Lan, J. H., Goldsmith, Y., Torfstein, A., Zhang, G. L., Zhang, J., Song, Y. P.,
910 Zhou, K. E., Tan, L. C., Xu, S., Xu, X. M., and Enzel, Y.: Dust storms in northern China
911 during the last 500 years, *Science China Earth Sciences*, 64, 813–824,
912 <https://doi.org/10.1007/s11430-020-9730-2>, 2021.
- 913 Zhang, Y., Shao, X. M., Yin, Z. Y., Liang, E. Y., Tian, Q. H., and Xu, Y.: Characteristics of
914 extreme droughts inferred from tree-ring data in the Qilian Mountains, 1700-2005, *Clim.
915 Res.*, 50, 141–159, <https://doi.org/10.3354/cr01051>, 2011.
- 916 Zhang, Y. X., Yu, L., and Yin, H.: Annual precipitation reconstruction over last 191 years at the
917 south edge of Badain Jaran Desert based on tree ring width data, *Desert and Oasis
918 Meteorology*, 9, 12–16 (In Chinese with English abstract),
919 <https://doi.org/10.3969/j.issn.1002-0799.2015.01.003>, 2015.
- 920 Zhang, Y. X., Gou, X. H., Hu, W. D., Peng, J. F., and Liu, P. X.: The drought events recorded
921 in tree ring width in Helan Mt. over past 100 years, *Acta Ecologica Sinica*, 25, 2121–2126
922 (In Chinese with English abstract), 2005b.
- 923